FRANK M. MONALDO

MEASUREMENTS OF DIRECTIONAL WAVE SPECTRA BY THE SHUTTLE SYNTHETIC APERTURE RADAR

During October 1984, measurements of directional ocean wave spectra in high sea states were made off the coast of Chile, near Tierra del Fuego, by a synthetic aperture radar aboard the space shuttle *Challenger*. Simultaneously, independent measurements of ocean wave spectra were made by a complement of airborne instruments. The results indicate that a low-altitude orbiting synthetic aperture radar would be a valuable supplement to existing operational wave forecasting models.

INTRODUCTION—THE NEED TO MEASURE OCEAN SURFACE WAVES

Ocean surface waves are a dominating factor for many activities at sea. The height, length, and propagation direction of waves can have a profound impact on the performance of ships and offshore platforms. The advantages of being able to predict the occurrence of unfavorable sea states are clear. Offshore platforms could be readied or evacuated in the face of menacing seas. Ships could chart optimum routes to lessen travel time and fuel consumption, and to increase safety. Even when safety is not an immediate problem, sea state conditions constrain the operational effectiveness of many naval systems. Thus, the ability to avoid limiting sea state conditions could significantly improve naval operational readiness.

The two-dimensional spectrum of ocean-wave height variance is the most complete descriptor of ocean surface waves, and it describes the directional distribution of wave energy at each wavelength and is important in calculating response functions of ships and towers. Numerically computed global forecasts of two-dimensional spectra are routinely provided to the Navy by the Fleet Numerical Oceanography Center. The numerical model currently uses ship-reported wind measurements to estimate the generation of surface waves and to propagate the waves forward in time and space.

Unfortunately, the accuracy of these forecasts is limited by the quality of the wind data that are put into the numerical forecast model. Wind measurements tend to be clustered around shipping routes, resulting in a paucity of data in the southern hemisphere, and are not always reliable.

At radar wavelengths of a few centimeters, ocean surface radar reflectivity is a measure of surface roughness, also on a scale of a few centimeters. Surface roughness on this scale, in turn, is sensitive to the local wind speed and direction. By measuring ocean surface radar reflectivity at different angles, instruments known as scatterometers are able to infer wind speed and direction. Spaceborne scatterometers, like the one aboard Seasat in 1978 and the one planned for the Navy Remote Ocean Sensing System in the early 1990s, promise to achieve global, reasonably consistent estimates of wind speed and direction.

Even with good wind inputs, reliable spectral model verifications are still inhibited by the lack of globally measured ocean wave spectra. Such measurements would permit the physics driving the numerical models to be tested on a large scale leading to model improvement. Intercomparisons among currently available wave forecast models suggest that, even for relatively simple wind conditions, there exists a wide range of projected wave spectra.[1] Global wave spectra estimates would also allow operational model outputs to be constrained and the model itself to be reinitialized, further improving subsequent forecasts.

THE SYNTHETIC APERTURE RADAR

An instrument thought to have the potential to measure ocean wave spectra on a global basis is the synthetic aperture radar (SAR). This high-resolution imaging radar concept was first developed by Goodyear in the early 1950s. After aircraft implementation of SAR and demonstration of the imaging of ocean surface waves,[2] a SAR was included as an experimental instrument aboard the Seasat satellite in 1978. Due to a power failure, the satellite functioned for only 100 days. However, so much high-quality SAR data was acquired in that brief period that 7 years later only a small fraction has been carefully examined.

Recent work at APL[3-5] and elsewhere[6,7] has clearly demonstrated the promise of SAR for measuring ocean waves. SAR ocean imagery in swaths 100 kilometers wide and 1000 kilometers long has been digitally processed to generate two-dimensional SAR image intensity spectra. Figure 1 provides an example of such a spectrum in polar coordinates in wavenumber, k (inverse wavelength), space. The outer circle corresponds to a 50-meter wavelength; the colors indicate SAR image-variance spectral density. The spectra are symmetric about the center, resulting in a 180-degree ambiguity. In Fig. 1, for example, the spectrum indicates that the longest wave system, the peak closest to the

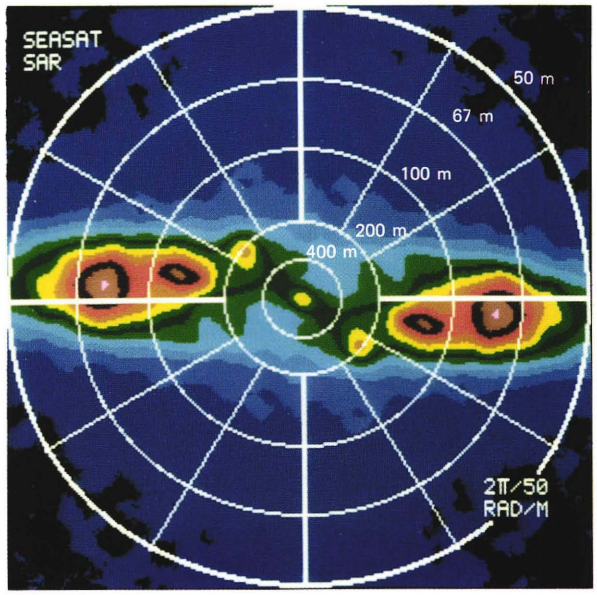

Figure 1—Example of Seasat SAR image intensity-variance spectrum. Vertical is the azimuth (along-satellite track) wavenumber direction. Horizontal is the range (cross-satellite track) wavenumber direction. Peaks in the spectrum represent concentrations of ocean wave energy.

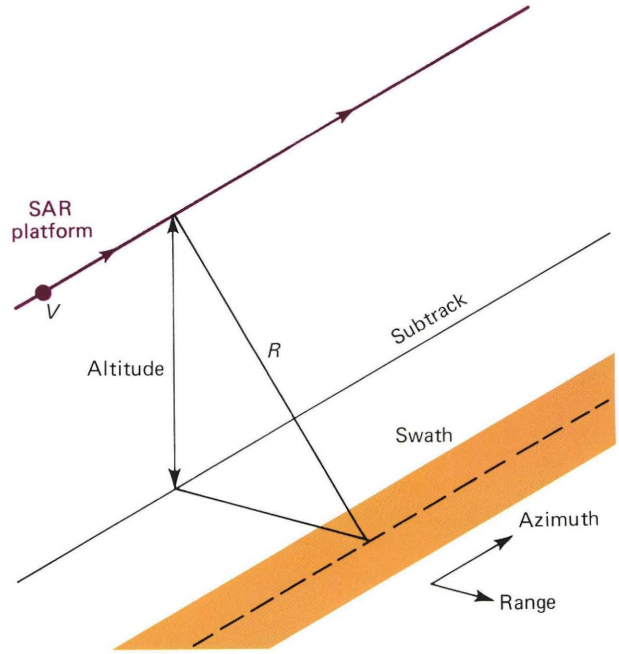

Figure 2—Generalized SAR geometry. For the Seasat SAR, the altitude was 800 kilometers; for the SIR-B mission, the altitude was 200 kilometers.

center, has a wavelength of 200 meters and is traveling −50 or 130 degrees from the SAR flight direction (straight up, in this spectrum).

Seasat SAR wave spectra are generally consistent with both numerical predictions of the wave field and limited independent measurements at the surface. However, few reliable independent estimates of the two-dimensional spectra were available in the Seasat era.

Unfortunately, the Seasat SAR spectra showed a systematic degradation in high sea states caused by moving scatterers on the ocean surface. To understand the nature of this problem requires a more complete description of how a SAR image is constructed. Elsewhere in this issue, Beal explains in greater detail the SAR imaging for a stationary scatterer. Basically, high cross-track or range resolution is provided by fine-scale timing measurements of a narrow transmitted pulse (see Fig. 2). The along-track or azimuth resolution for a conventional radar is limited by the beamwidth of the antenna.

High azimuth resolution for a SAR is obtained by examining the Doppler shift in the return radar signal. As a SAR passes over a scatterer, the relative velocity between the scatterer and the SAR platform (and hence the Doppler shift of the return signal) changes. When the SAR is far from the scatterer, the relative velocity is equal to the SAR platform ground-track velocity, V. As the SAR platform approaches, the relative velocity decreases and becomes zero when the azimuth position of the SAR platform and the scatterer are equal. It is at this point (zero relative velocity and zero Doppler shift) that the azimuth position of the scatterer is assigned in a SAR image.

A moving scatterer changes this situation. Because the velocity of the scatterer is added to the SAR platform velocity, the azimuth position of zero relative motion and zero Doppler is now shifted. The scatterer appears displaced in the SAR image. For example, SAR images over land have shown moving trains offset from stationary train tracks. This azimuth position shift, Δx, is given by

$$\Delta x = \frac{R}{V} v_r \, , \tag{1}$$

where R is the minimum range between the SAR platform and the scatterer, V is the satellite ground-track velocity, and v_r is the component of scatterer velocity parallel to the radar beam.

This positional shift of scatterers tends to degrade the resolution of SAR wave imagery. On the ocean surface, scattering elements are randomly advected by the vertical and horizontal motion of the water, causing random azimuth position shifts. The resulting SAR image is smeared in the azimuth direction, effectively defocusing azimuth traveling waves.

This problem, first clearly identified in Seasat SAR ocean imagery, is particularly acute during high sea states, precisely the time when wave spectra are of most interest. Referring again to Fig. 1, note that at high azimuth wavenumbers the spectral response is extremely diminished. This illustrates the manifestation of azimuth smear in the SAR image spectrum.

A simple empirical relation proposed for the minimum detectable azimuth wavelength, λ_m, as a function of significant wave height, H_s, is given in Ref. 8:

$$\lambda_m \cong 1 \left(\frac{\text{meters}^{1/2}}{\text{seconds}} \right) \frac{R}{V} H_s^{1/2} \, . \tag{2}$$

Significant wave height is defined as the minimum height of the highest one-third of the waves. For a typical significant wave height of 3 meters, the minimum detectable azimuth wavelength is 210 meters for the Seasat SAR configuration.

Thus, 7 years of Seasat SAR analysis have yielded the following:

1. Spaceborne SARs clearly hold the potential for providing global wave spectra. The wavelength and propagation direction of SAR-measured ocean wave systems are generally in good agreement with both independent measurements and ocean wave model predictions.
2. No Seasat data set exists for which high-quality spaceborne SAR image spectra can be quantitatively compared with independent measurements of full two-dimensional ocean wave spectra that have a spectral resolution comparable to the SARs. As a consequence, the potential benefit of updating wave forecasts with SAR image spectra had not been demonstrated. In principle, the integration of actual ocean wave spectra could not but help to improve such forecasts. The question remained, however, as to how much improvement would accrue with the inclusion of SAR-derived wave spectra.
3. Seasat SAR data clearly showed systematic azimuth wavenumber degradation at high sea states. It was hypothesized that such degradation was a function only of the ocean sea state and the R/V ratio of the SAR platform.

SIR-B—AN OPPORTUNITY

In October 1984, the Shuttle Imaging Radar (SIR-B) mission (see Beal's article in this issue) provided an opportunity to address unresolved issues concerning the ability of a spaceborne SAR to monitor ocean waves on a global scale.

The intervening years between Seasat and SIR-B allowed the maturation of two airborne instruments capable of measuring the full two-dimensional ocean wave spectrum with high wavelength and angular resolution: the surface contour radar and the radar ocean wave spectrometer. These instruments will be described later.

With these new instruments, we can compare independent measurements of the ocean wave spectra coincident in time and space with shuttle SAR-derived wave spectra measurements. Any systematic biases in the SAR spectra can be examined and methods of correcting them devised. In addition, SAR image intensity values might be calibrated against surface height or slope measurements made by the other instruments.

Since the shuttle altitude (and thus the R/V ratio) is only about one fourth that of Seasat (200 versus 800 kilometers), the SIR-B mission provided an opportunity to test the prediction that the ocean surface motion problem would be alleviated, also by a factor of four. For a 3-meter significant wave height, the minimum detectable azimuth wavelength would be 50 meters, compared to 200 meters for Seasat. The clear implication would be that future SAR missions dedicated to measuring ocean waves should be placed in a low-altitude orbit.

Although the physical ideas behind wave generation models have not changed substantially since the 1970s, the numerical implementation of these models has improved. In particular, by 1984, the Fleet Numerical Oceanography Center had implemented an improved numerical forecast model (the Global Spectral Ocean Wave Model) that routinely provides wave forecasts over the entire world. These model forecasts invite direct intercomparisons with spectra obtained from SIR-B.

THE CHILE EXPERIMENT

The Chile experiment provided an opportunity to compare SAR wave imagery with measurements of ocean wave spectra from the airborne surface contour radar and the radar ocean wave spectrometer. At the time of year of the SIR-B mission, the desirable high sea states were much more likely to be found in the southern hemisphere. Therefore, the airborne portion of the experiment was based in Punta Arenas, Chile, located on the Straits of Magellan, at about 53 degrees south latitude.

The NASA P-3 aircraft used for the experiment was equipped with four instruments capable of measuring at least some aspect of the two-dimensional ocean wave spectrum: the surface contour radar, the radar ocean wave spectrometer, the advanced airborne flight experiment altimeter, and an airborne optical lidar. For five days, October 8 through 12, 1984, the P-3 aircraft flew flight paths coincident with the acquisition of SAR imagery from the shuttle, while acquiring ocean wave spectral data. Figure 3 is a schematic representation of the experiment. Figures 4a and 4b provide examples of the relative positions of P-3 aircraft data acquisition areas and SAR swaths during the experiment.

The surface contour radar and the radar ocean wave spectrometer both provide estimates of the full two-dimensional ocean wave spectrum. The surface contour radar is basically a high-resolution radar altimeter. As the plane flies forward, a pencil radar beam scans laterally, measuring the distance between the airplane and the surface to create an ocean surface elevation map (see Fig. 5). This map is then Fourier-transformed and squared to generate a two-dimensional wave height-variance spectrum.[9]

The radar ocean wave spectrometer uses a conically scanning, narrow pulse beam at near-vertical incidence. When pointing in one direction, the beam returns a signal proportional to the slope variation of the ocean surface along that direction. The square of the Fourier transform provides the ocean surface slope-variance as a function of wavenumber along the antenna look direction. The combination of similar spectra formed by a complete conical rotation of the antenna results in a full two-dimensional ocean slope-variance spectrum (see Fig. 6). Subsequently, this

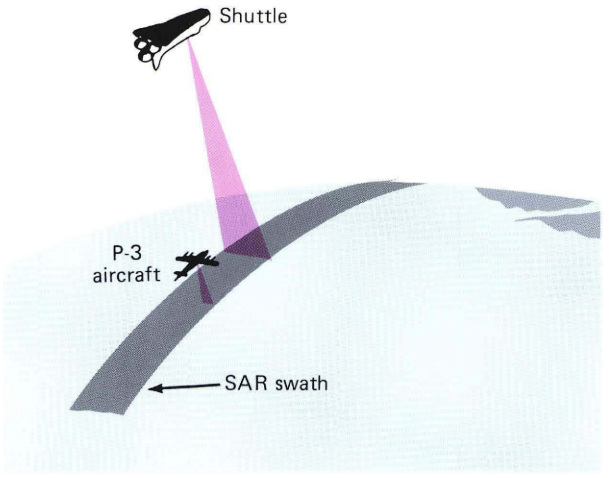

Figure 3—Schematic depiction of the Chile experiment with shuttle imaging radar and independent measurements made from a P-3 aircraft.

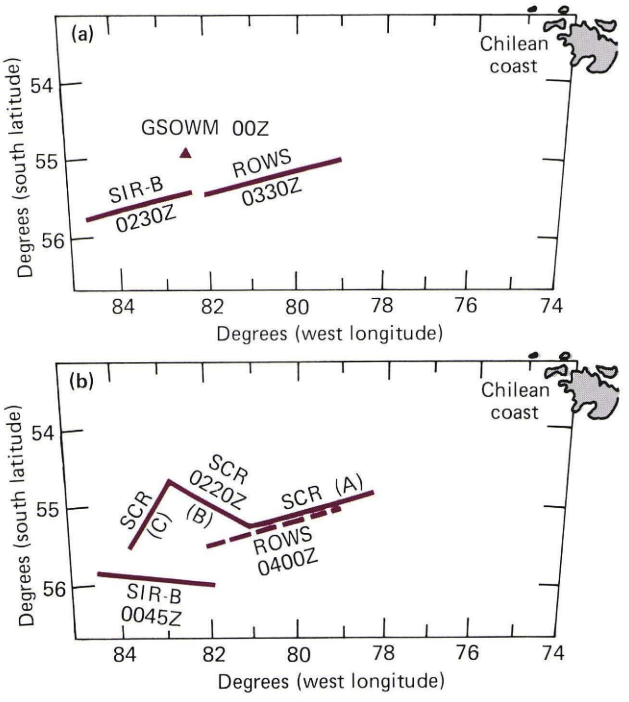

Figure 4—Positions of SAR swath measurement areas for P-3 sensors and the GSOWM (Global Spectral Ocean Wave Model) grid point. (ROWS is the radar ocean wave spectrometer; SCR is the surface contour radar.) (a) SIR-B and ROWS measurement locations for October 11, 1984, with respect to the nearest GSOWM grid point. (b) SIR-B, ROWS, and SCR measurement locations for October 12, 1984; GSOWM was inoperative; (A), (B), and (C) indicate flight lines.

slope-variance spectrum can be converted to the corresponding height-variance spectrum.[10]

The other two instruments do not yield full two-dimensional spectra but do provide independent and important measures of it. The advanced airborne flight experiment altimeter uses the spreading of the return

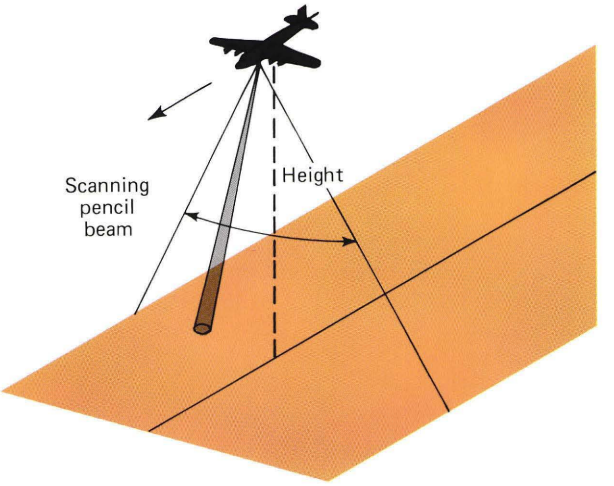

Figure 5—The surface contour radar scans laterally using a pencil beam to measure the distance to the surface.

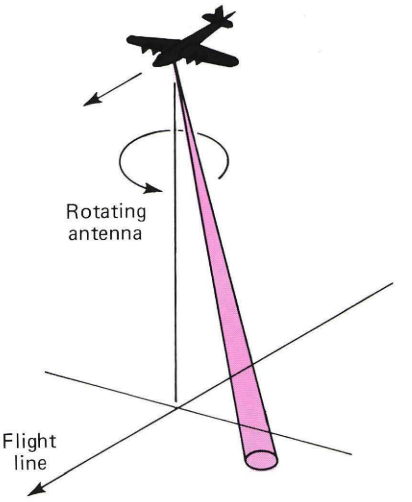

Figure 6—The radar ocean wave spectrometer uses a conically scanning antenna to measure ocean surface slope variations.

radar pulse of a nadir-looking altimeter by ocean surface waves to estimate the total wave height variance. This number is equal to the integral of the full two-dimensional wave height-variance spectrum over wavenumber and angle. The airborne optical lidar is a profiling lidar that allows the determination of a one-dimensional height-variance spectrum along the aircraft's flight line.

Unfortunately, during the shuttle flight, problems aboard *Challenger* severely limited the amount of SAR data recorded. Because of the high data rates associated with a SAR, it was originally planned that the SAR data would be relayed to a high data rate relay satellite, the Tracking and Data Relay Satellite (TDRS), and then to ground stations. The servomechanisms on the shuttle data-transmission antenna malfunctioned, however, making it impossible simultaneously to ac-

quire SAR data and relay the data through TDRS back to a ground station.

To alleviate the problem, SAR data were recorded on digital tapes aboard the shuttle. Subsequently, the entire shuttle was rotated so the data transmission antenna would point toward TDRS and transmit the recorded data. Although this fix permitted the acquisition of SAR data, only a fraction of the data originally anticipated could be obtained.

Since the Chile experiment was conducted in the southern hemisphere, there was less potential conflict with other investigators in scheduling SAR data acquisition. Five days of high-quality digital SAR data were acquired coincident with underflights by the P-3 used in our experiment. This was less than expected, but more than enough to address the questions that originally prompted the experiment.

PRELIMINARY RESULTS

Although the wave spectra derived from the various instruments have not yet been fully analyzed, substantial agreement between the measurements has already been realized.[11] We have chosen to concentrate the preliminary analysis on comparisons among the ocean wave spectra from various instruments and the numerically predicted spectra for the last two days of data collection, October 11 and 12, 1984.

On October 12, all three instruments capable of measuring full two-dimensional wave spectra were operating: the SAR, the radar ocean wave spectrometer, and the surface contour radar. Unfortunately, the Fleet Numerical Oceanography Center wave forecast model was inoperative for that particular day. Figure 4b shows the flight path of the P-3 aircraft on October 12 and indicates the regions where its various sensors were operating with respect to the SAR imagery. On October 11, the Fleet Numerical Oceanography Center wave forecast model was operative but the surface contour radar was not. Nonetheless, we are able to compare numerically predicted spectra with actual two-dimensional spectra measured from two independent instruments: the SAR and the radar ocean wave spectrometer.

On October 12, the advanced airborne flight experiment altimeter and the airborne optical lidar measured a significant wave height of 3.5 meters. Figure 7 shows a comparison of measured two-dimensional spectra from that day. The surface contour radar obtains its best spectral resolution in the direction parallel to the flight path. Therefore, optimal surface contour radar spectra are determined by examining individual spectra from several flight directions. Figure 7a shows the height-variance spectrum from the surface contour radar obtained from a single aircraft heading. The composite height-variance spectrum from three aircraft headings is shown in Fig. 7b.

Spectra from the radar ocean wave spectrometer are shown in Figs. 7c and 7d. The spectrometer provided a direct estimate of the two-dimensional ocean slope-variance spectrum, shown in Fig. 7c. Figure 7d shows the ocean height-variance spectrum inferred from the

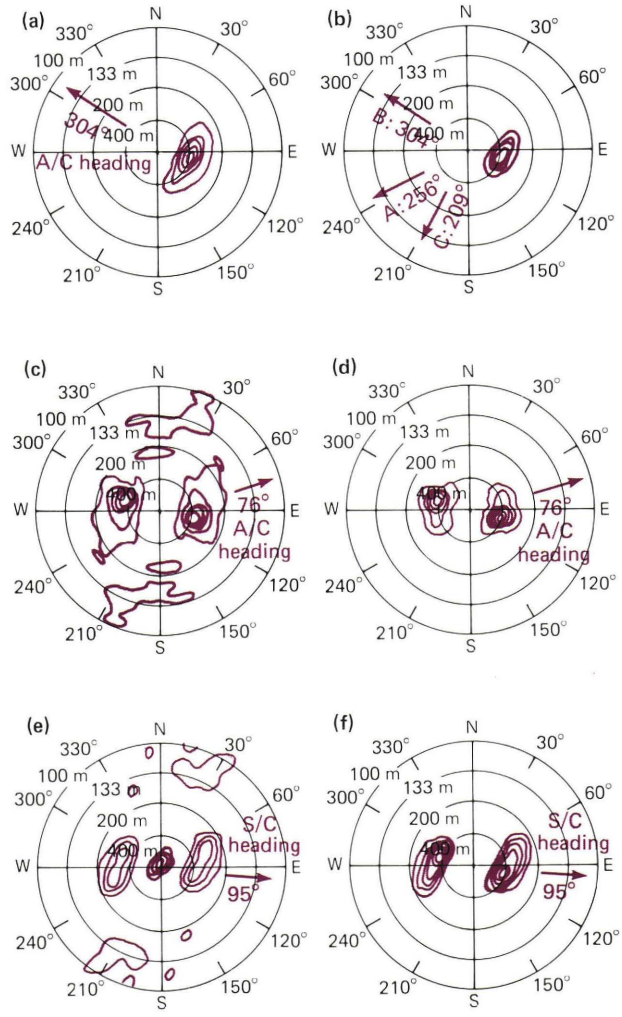

Figure 7—Wave spectra for October 12, 1984: (a) surface contour radar (SCR) height-variance spectrum along flight line B (see Fig. 4b); (b) SCR height-variance spectrum from flight lines A, B, C (see Fig. 4b); (c) radar ocean wave spectrometer (ROWS) slope-variance spectrum (55.5°S, 81.5°W, 0400 GMT); (d) ROWS height-variance spectrum (55.5°S, 81.5°W, 0400 GMT); (e) SIR-B SAR intensity-variance spectrum (56.0°S, 82.0°W, 0045 GMT); (f) SIR-B SAR intensity-variance spectrum $\times$ $1/k^2$ (56.0°S, 82.0°W, 0045 GMT).

slope spectrum. Note the general agreement in the wavenumber and propagation direction of the dominant peak in both the surface contour radar and radar ocean wave spectrometer spectra. The surface contour radar spectral peak, however, appears somewhat more elongated than the spectrometer peak.

SAR image intensity is not a direct measure of ocean surface slope or height but rather of its radar cross section. The relationship between image radar cross section and ocean slope or height is not well understood. The consensus, however, is that SAR image intensity is closely related to surface slope.

SAR image spectra for October 12 are shown in Figs. 7e and 7f. The original SAR image spectrum in Fig. 7e closely resembles the slope-variance spectrum

measured by the radar ocean wave spectrometer. Encouraged by this close correspondence between the SAR image intensity-variance spectrum and the spectrometer slope-variance spectrum, we then computed the corresponding height-variance spectrum, as shown in Fig. 7f. This SAR-derived height-variance spectrum is very similar to both the spectrometer and the surface contour radar spectra. In fact, the differences between the measured spectra are probably consistent with the actual spatial variability of the ocean surface between the patches in which the spectra were measured.

On October 11, the advanced airborne flight experiment altimeter and the airborne optical lidar indicated that the significant wave height was about 4 meters. Figure 4a depicts the flight path of the P-3 with respect to the position of SAR imagery.

Figures 8a and 8b show, respectively, the slope- and height-variance spectra obtained from the radar ocean wave spectrometer on October 11. The SAR-derived wave slope- and height-variance spectra from a patch of imagery almost exactly coincident, spatially and temporally, with the area measured by the spectrometer are shown in Figs. 8c and 8d, respectively. The similarity between these two spectra is remarkable. They are essentially identical.

As the spectral data from the SIR-B SAR and the P-3 instrumentation are more and more carefully examined and processed, it is becoming clearer that SAR image spectra can be systematically processed to provide reliable estimates of the two-dimensional height-variance spectrum.

Comparison of these spectra with wave forecast model predictions for October 11 also reveals some interesting similarities and differences. Figures 8c and 8d depict wave height-variance spectra predicted by the Fleet Numerical Oceanography Center in the vicinity of the SAR imagery and the P-3 flight path.

Figure 8e represents the center's spectrum at 82.5 degrees west longitude and 55 degrees south latitude, the grid point closest to the measured spectra. Although it is generally similar to the measured spectra, the spectrum in Fig. 8f seems more similar despite the fact that its position, 82.5 degrees west longitude and 52.5 degrees south latitude, is farther from the measured spectra. A simple mislocation of the generating wind fields used to derive the center's forecasts may account for this discrepancy.

Although a more thorough comparison between the forecasted and the measured spectra needs to be made, it seems that SAR-derived wave spectra are sufficiently accurate to be used to update and correct numerical model outputs. A closer examination of the numerically predicted spectra reveals that they have substantially more angular width than either the SAR or the spectrometer's spectra. This suggests a way in which model spectra might be in error.

One of the more important results of the experiment thus far is the notable reduction of azimuth smearing in the SAR imagery. Compare the SAR spectrum shown in Fig. 1, from Seasat for the modest significant wave height of 1 meter, with the spectrum in Fig. 9, from SIR-B for the significant wave height of 3.5 meters. The characteristic falloff in azimuth response at high wavenumber is not present in the SIR-B spectrum, confirming the hypothesis that a reduction of the range-to-velocity ratio of the SAR platform reduces the azimuth smearing.,

Note, however, that the response at high range wavenumber in the SIR-B SAR spectrum is reduced compared to Seasat. This loss of range resolution was an expected result from a reduction of the SAR bandwidth in SIR-B. It does not reflect a fundamental limitation of SAR ocean imagery but is purely a consequence of hardware limitations specific to the SIR-B SAR.

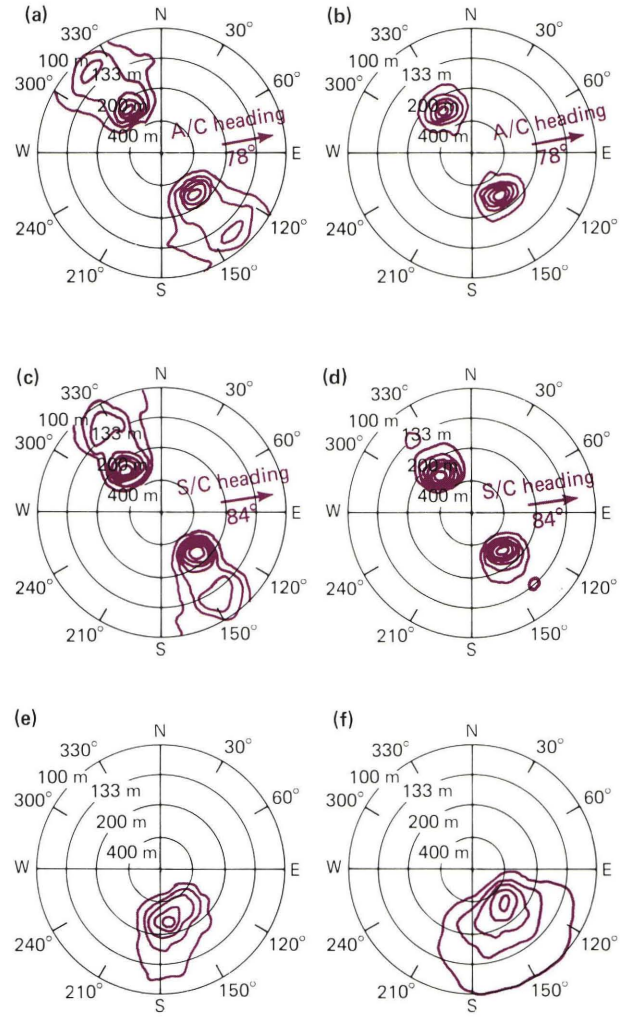

Figure 8—Wave spectra for October 11, 1984: (a)radar ocean wave spectrometer (ROWS) slope variance spectrum (55.3°S, 81.2°W, 0330 GMT); (b) ROWS height-variance spectrum (55.3°S, 81.2°W, 0330 GMT); (c) SIR-B SAR intensity-variance spectrum (55.5°S, 82.5°W, 0230 GMT); (d) SIR-B SAR intensity-variance spectrum × $1/k^2$ (55.5°S, 82.5°W, 0230 GMT); (e) Global Spectral Ocean Wave Model (GSOWM) height-variance forecast (55.0°S, 82.5°W, 0000 GMT); (f) GSOWM height-variance forecast (55.0°S, 82.5°W, 0000 GMT).

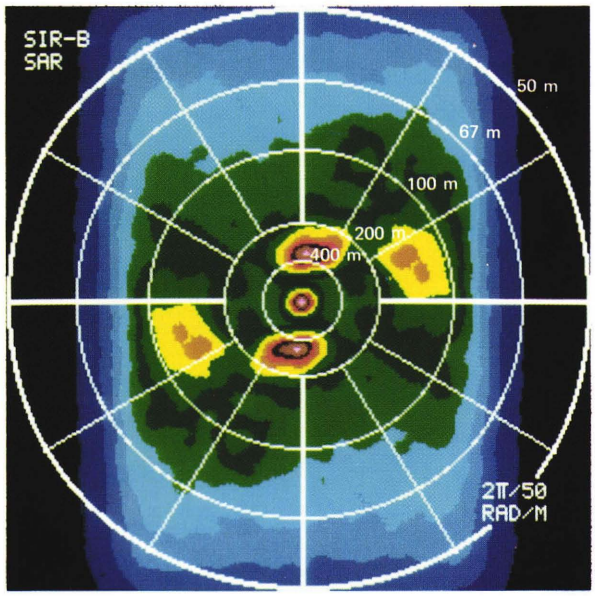

Figure 9—Example of SIR-B SAR image intensity-variance spectrum. Vertical is the azimuth wavenumber direction. Horizontal is the range wavenumber direction.

CONCLUSIONS

There are three preliminary conclusions to be drawn from the SIR-B experiment off the coast of Chile:

1. Comparison with the radar ocean wave spectrometer suggests that the SAR image intensity-variance spectrum of range-traveling waves is most closely associated with the ocean slope-variance spectrum. No systematic biases between the spectrometer and the SAR spectra are yet evident. However, a precise calibration between SAR intensity-variance spectra and slope-variance spectra still needs to be made.
2. The azimuth resolution limitations induced by ocean surface motion that are inherent in Seasat imagery are substantially reduced by using a low-altitude SAR.
3. Numerical wave modeling predictions of the ocean spectra, although generally consistent with measured ocean wave spectra, can be substantially biased. Such errors could potentially be reduced by complementing predictions with measured spectra.

Thus far, we have examined a relatively small portion of the data available for analysis. The above conclusions will, no doubt, be influenced by both a more intensive and a more inclusive examination of the data.

REFERENCES

[1] "An Intercomparison Study of a Wind Wave Prediction Model," SWAMP (Sea Wave Modeling Project), *Wave Dynamics and Radio Probing of the Ocean Surface,* O. M. Phillips and K. Hasselmann, eds., Plenum Press (in press, 1985).

[2] C. Elachi and W. E. Brown, "Models of Radar Imaging of Ocean Surface Waves," *IEEE Trans. Antennas Propag.* **AP-25**, 84-95 (1977).

[3] R. C. Beal, D. G. Tilley, and F. M. Monaldo, "Large- and Small-Scale Spatial Evolution of Digitally Processed Ocean Wave Spectra from the Seasat Synthetic Aperture Radar," *J. Geophys. Res.* **88**, 1761-1778 (1983).

[4] R. C. Beal, T. W. Gerling, D. E. Irvine, F. M. Monaldo, and D. G. Tilley, "Spatial Variations of Ocean Wave Directional Spectra from the Seasat Synthetic Aperture Radar," *J. Geophys. Res.* (in press, 1985).

[5] F. M. Monaldo, "Improvement in the Estimate of Dominant Wavenumber and Direction from Spaceborne SAR Image Spectra When Corrected for Ocean Surface Movement," *IEEE Trans. Geosci. Remote Sensing* **GE-22**, 603-608 (1984).

[6] W. R. Alpers, D. B. Ross, and C. L. Rufenach, "On the Detectability of the Ocean Surface Waves by Real and Synthetic Aperture Radar," *J. Geophys. Res.* **86**, 6481-6498 (1981).

[7] R. A. Shuchman, J. D. Lyden, and D. R. Lyzenga, "Estimates of Ocean Wavelength and Direction from X- and L-Band Synthetic Aperture Radar Data During the Marineland Experiment," *IEEE J. Oceanic Eng.* **OE-8**, 90-96 (1983).

[8] F. M. Monaldo and R. C. Beal, "Limitations of the Seasat SAR in High Sea States," *Wave Dynamics and Radio Probing of the Sea Surface,* O. M. Phillips and K. Hasselmann, eds., Plenum Press (in press, 1985).

[9] E. J. Walsh, D. W. Hines III, R. N. Swift, and J. F. Scott, "Directional Wave Spectra Measured with the Surface Contour Radar," *J. Phys. Oceanogr.* **15**, 566 (1985).

[10] F. C. Jackson and W. T. Walton, "Aircraft and Satellite Measurement of Ocean Wave Directional Spectra Using Scanning-Beam Microwave Radars," *J. Geophys. Res.* **90**, 987-1004 (1985).

[11] R. C. Beal, F. M. Monaldo, D. G. Tilley, D. E. Irvine, E. J. Walsh, F. C. Jackson, D. W. Hancock III, D. E. Hines, R. N. Swift, F. I .Gonzalez, D. R. Lyzenga, and L. F. Zambresky, "A Comparison of SIR-B Directional Ocean Wave Spectra with Aircraft Scanning Radar Spectra and Global Spectral Ocean Wave Model Predictions," *Science* (in press, 1985).

ACKNOWLEDGMENT—Many individuals were involved in the execution of the experiment described in this paper. Besides the experiment team both in the United States and in Chile, the local Chilean people and authorities as well as the shuttle crew share a large measure of the credit for the success of the experiment.

THE AUTHOR

FRANK M. MONALDO was born in Washington, D.C., in 1956 and received the B.A. and M.S. degrees, both in physics, from the Catholic University of America in 1977 and 1978, respectively. Employed at APL since 1977, he has concentrated on various areas of remote sensing, particularly the remote sensing of ocean surface features. In 1980, he was a visiting scientist at the Max Planck Institute of Meteorology in Hamburg, West Germany. His work at APL has included optical imaging of ocean phenomena from near-surface platforms, as well as synthetic aperture radar imaging of the ocean surface from spaceborne platforms. Mr. Monaldo is also involved in the evaluation of potential errors that arise in spaceborne altimetry and in the development of advanced altimeter design concepts. Current activities are focused on the study of data from the recent shuttle SAR mission and the Geosat radar altimeter. He is a member of the Phi Beta Kappa and Blue Key honor societies and the American Geophysical Union.